



# Co(OH)<sub>2</sub> Nanosheets Supported on Laser Ablated Cu Foam: An Efficient Oxygen Evolution Reaction Electrocatalyst

Xinfeng Zhou<sup>1</sup>, Weihong Qi<sup>1,2\*</sup>, Kai Yin<sup>3</sup>, Ning Zhang<sup>1</sup>, Shen Gong<sup>1</sup>, Zhou Li<sup>1</sup> and Yejun Li<sup>1,3\*</sup>

<sup>1</sup> School of Materials Science and Engineering, Central South University, Changsha, China, <sup>2</sup> State Key Laboratory of Solidification Processing, Center of Advanced Lubrication and Seal Materials, Northwestern Polytechnical University, Xi'an, China, <sup>3</sup> Hunan Key Laboratory of Super Microstructure and Ultrafast Process, School of Physics and Electronics, Central South University, Changsha, China

## OPEN ACCESS

### Edited by:

Chundong Wang,  
Huazhong University of Science and  
Technology, China

### Reviewed by:

Qiaobao Zhang,  
Xiamen University, China  
Ruguang Ma,  
Shanghai Institute of Ceramics (CAS),  
China

### \*Correspondence:

Weihong Qi  
qihw216@nwpu.edu.cn  
Yejun Li  
yejunli@csu.edu.cn

### Specialty section:

This article was submitted to  
Electrochemistry,  
a section of the journal  
Frontiers in Chemistry

**Received:** 07 November 2019

**Accepted:** 13 December 2019

**Published:** 10 January 2020

### Citation:

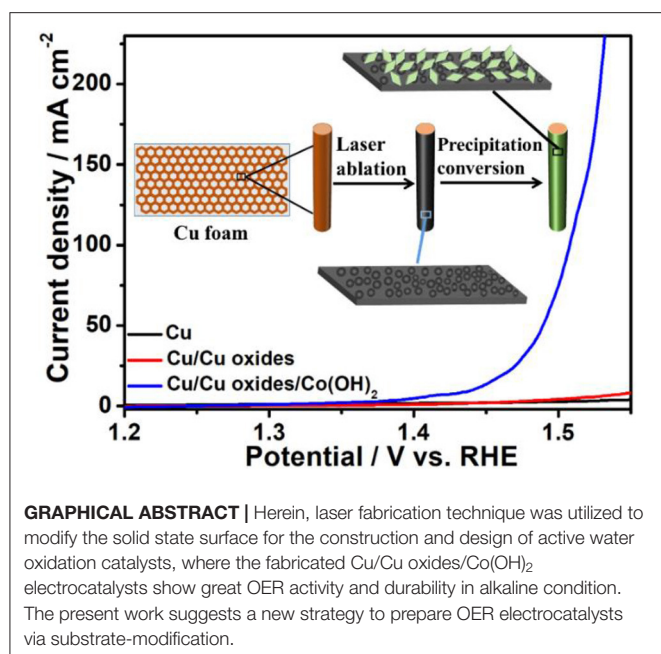
Zhou X, Qi W, Yin K, Zhang N,  
Gong S, Li Z and Li Y (2020) Co(OH)<sub>2</sub>  
Nanosheets Supported on Laser  
Ablated Cu Foam: An Efficient Oxygen  
Evolution Reaction Electrocatalyst.  
*Front. Chem.* 7:900.  
doi: 10.3389/fchem.2019.00900

Highly efficient and low-cost non-noble metal based electrocatalysts for oxygen evolution reaction (OER) have attracted more and more attention in recent years. However, the current research has been focused on the construction of novel OER electrocatalysts themselves, little attention has been paid to the modification of the substrates. In this work, a different strategy is proposed via laser ablation to fabricate the Cu foams with rich micro/nano-structures as OER substrates. Later, the precipitation conversion method was utilized to grow cobalt hydroxide on the laser fabricated Cu foams. The as-produced Cu/Cu oxides/Co(OH)<sub>2</sub> electrocatalysts exhibit high OER activity in 1 M KOH, requiring an overpotential of only 259 mV at a current density of 50 mA cm<sup>-2</sup> with excellent mid-term durability. The improved catalytic performance of the prepared samples can be attributed to the increased surface area, rich active sites, and the superhydrophilicity of the laser produced micro/nano-structures.

**Keywords:** laser fabrication, electrocatalysis, sustainable chemistry, transition metal oxide, water splitting

## INTRODUCTION

As a high-power density and zero carbon emission renewable energy carrier, hydrogen (H<sub>2</sub>) has been considered as an ideal alternative energy of fossil fuels (Li et al., 2016, 2019a; Shi and Zhang, 2016; Jin J. et al., 2017; Meng et al., 2017). Electrochemical water splitting has been suggested as an effective approach to produce hydrogen, which has attracted tremendous interests. However, the efficiency of the electrochemical water splitting is greatly hindered by oxygen evolution reaction (OER), which contains a complicated progress of 4H<sup>+</sup>/4e<sup>-</sup> transfer with sluggish reaction kinetics (Gong et al., 2013; Lu et al., 2016; Ma et al., 2016; Xia et al., 2016; Wu et al., 2017; Lv et al., 2019). Therefore, water oxidation catalysts are needed to lower the OER overpotential, such as noble metal-based catalysts (ruthenium and iridium), which, however, are restricted from widespread industrial application due to the limited supply and high price (Lee et al., 2012; Ai et al., 2017). To satisfy the industrial demand, it is of great importance to develop high efficient OER electrocatalysts based on non-noble metals in the future.



In recent years, transition metals, such as copper and nickel foams, have been widely used as substrates of electrocatalysts for efficient water splitting, due to the low cost, high conductivity, and large surface area. For example, Xiong et al. reported the Co-doped CuO nanoarrays on Cu foam as the efficient and stable anode for electrochemical water splitting, with an overpotential of 299 mV at current densities of 50 mA cm<sup>-2</sup> (Xiong et al., 2018). A 3D OER electrocatalyst with Cu(OH)<sub>2</sub>@CoCO<sub>3</sub>(OH)<sub>2</sub>·nH<sub>2</sub>O heterostructures on Cu foam has been developed by Xie et al. (2017), exhibiting high OER activity with only 290 mV to achieve 100 mA cm<sup>-2</sup> in 1 M KOH. Hierarchical NiCo<sub>2</sub>S<sub>4</sub> nanowire arrays have been grown on Ni foam as bifunctional electrocatalysts for both oxygen and hydrogen evolution reactions, which shows stable catalytic activity with overpotentials of 260 mV and 210 mV for OER and HER in 1 M KOH, respectively (Sivanantham et al., 2016).

Despite of these efforts, the current research has been focused on the construction of novel OER electrocatalysts themselves, while little attention has been paid to the modification of the substrates. Laser fabrication has been suggested as an effective approach to modify the solid surface with rich micro/nano-structures, large surface area, and rich defects, as well as superhydrophilicity (Yin et al., 2017a; Yang et al., 2018; Li et al., 2019b; Wu et al., 2019). For Cu foams, the produced Cu oxides have been found to be active in OER (Li et al., 2019b). Moreover, the modified Cu surface with rich micro/nano-structures can be beneficial to the growth of the electrocatalysts as well as to the release of the produced O<sub>2</sub> gas, thus increase the active sites as well as the catalytic activity. Furthermore, the laser ablation can be a surface fabrication process by adjusting the laser parameters, where the metallic Cu core can be largely retained as the conductive substrate. It is therefore of great interests to combine the laser modified substrates with the electrocatalysts to promote the OER process.

In this contribution, femtosecond laser ablation was utilized to fabricate rich micro/nano-structures on Cu foam, while cobalt hydroxide was grown on the fabricated Cu foam via the precipitation conversion method. The as-prepared electrocatalysts exhibited remarkable OER activity and excellent mild-term stability.

## EXPERIMENTAL SECTION

### Materials and Chemicals

All chemicals and metal salts including potassium hydroxide (KOH), Sodium dodecyl sulfate (SDS), carbamide (CO(NH<sub>2</sub>)<sub>2</sub>), and cobalt chloride (CoCl<sub>2</sub>·6(H<sub>2</sub>O)) were purchased from Aladdin Co., Ltd., and used without further purification.

### Fabrication of Cu Oxides Micro/Nanostructures on Cu Foam

The copper foam was purchased from Kunshan Metal Material Tech., Suzhou, China. The typical line-by-line femtosecond laser irradiation procedure is applied to modify the Cu foam, where detailed information can be found in previous work (Yin et al., 2017b; Duan et al., 2018). In particular, a high-repetition femtosecond laser system (PHAROS, LIGHT CONVERSION, Lithuania) that generates 250 fs pulses at a repetition rate of 75 kHz with a central wavelength of 1,030 nm is employed to fabricate micro/nano structures on the Cu foam surface. The spacing between two adjacent lines is set to be 10 μm. The laser power and speed were set at 8 W and 3 m/s (about 4 s), respectively. After ablation, the samples were carefully cleaned with distilled water.

### Preparation of the Cu/Cu Oxides/Co(OH)<sub>2</sub>

The Cu/Cu oxides/Co(OH)<sub>2</sub> electrodes were prepared via the precipitation conversion method (Jin H. et al., 2017). In a typical procedure, a 0.23 g mixture of CoCl<sub>2</sub> · 6H<sub>2</sub>O (40 mg), urea (120 mg), and SDS (120 mg) were added into a Teflon-lined autoclave containing 16.7 mL water to form a suspension. After a few minutes stirring, the laser fabricated Cu foam was immersed into the suspension, which was latter placed into a homogeneous reactor at 120°C for a different amount of time (2, 4, 6, 8, and 10 h). Eventually, the products were cooled in air and washed repeatedly with ethanol, followed by drying in vacuum. The mass loading of Co(OH)<sub>2</sub> catalysts on the laser ablated Cu foam (Cu/Cu Oxides/Co(OH)<sub>2</sub>-8 h) is estimated based on EDS results, i.e., 10.21 mg/cm<sup>2</sup>.

### Materials Characterizations

X-ray diffraction (XRD) was performed on a Mini Flex 600 using Cu Kα radiation (λ = 0.1542 nm) with a scan rate of 2° min<sup>-1</sup>. The morphologies of the samples were recorded by a Mira3 scanning electron microscope (SEM) and transmission electron microscope (TEM) images were obtained on Tecnai G2 F20 instruments operating at an accelerating voltage of 200 kV. The elemental composition and the valence states of the samples were detected by X-ray photoelectron spectroscopy (XPS) on SPECS ultrahigh vacuum system (Liu et al., 2015, 2019; Xie et al., 2016).

## Electrochemical Measurements

All electrochemical measurements were carried out with a Chenhua CHI 760E electrochemical workstation using a standard three-electrode system in 1 M KOH solution (pH 13.8) at room temperature. The prepared samples, a graphite rod, and a Hg/HgO electrode were used as the working electrode, counter electrode, and reference electrode, respectively. The linear sweep voltammograms (LSVs) were measured at a scan rate of  $5 \text{ mV s}^{-1}$  with iR compensations, where the Tafel slope can be derived from. The electrochemical impedance spectroscopy (EIS) measurement was performed at an electrolysis potential of 1.5 V vs. RHE over a frequency range from 0.01 to 100 kHz with ac amplitude of 5 mV. A simplified Randles equivalent circuit was used to simulate the Nyquist plot. The capacitance (normalized by the area) was determined from the cyclic voltammetry (CV) scans. The CV scans with various scan rates (5, 10, 20, 40, 80, 120, 160, and  $200 \text{ mV s}^{-1}$ ) were recorded in a non-faradaic potential range (0–0.1 V vs. Hg/HgO). The full water splitting measurements is carried out with a membrane to separate the  $\text{H}_2$  and  $\text{O}_2$ , where the LSV curves are not iR corrected. The distance between the two electrodes is about 5 cm. Faradaic efficiency was measured toward gas chromatography experiment (GC-2014C, SHIMADZU) and the Faradaic efficiency of Cu/Cu Oxides/Co(OH)<sub>2</sub>-8 h is about 98.4%. All potentials measured in this work were converted to reversible hydrogen electrode (RHE)

scale using the Nernst equation:  $E_{\text{RHE}} = E_{\text{Hg/HgO}} + 0.059 \times \text{pH} + 0.098$ . The overpotential is estimated by  $E_{\text{RHE}} - 1.23$ .

## RESULTS AND DISCUSSIONS

The morphology evolution from the pristine Cu foam, over laser ablation, to precipitation conversion was demonstrated by SEM and TEM characterizations. As shown in **Figure 1**, the smooth Cu surface turns to be with rich micro/nano-structures after laser ablation, which are composed of nanoparticles with a size of a few to a few tens of nanometers (**Figure 1e**). The HRTEM images of the laser fabricated Cu foam show lattice spacing of 0.246, 0.213, and 0.232 nm, corresponding to Cu<sub>2</sub>O (111), Cu<sub>2</sub>O (200), and CuO (111), respectively (**Figure 1f**), which suggests the oxidization of the Cu surface after laser ablation. These micro/nano-structures significantly increase the surface area with rich defects and superhydrophilicity (Li et al., 2019a), which can be beneficial to the growth of the electrocatalysts and increases the active sites as well as the catalytic activity. To compare the specific surface area of the Cu foam before and after the laser ablation, we conducted Brunauer-Emmett-Teller (BET) measurements of the fabricated samples. It shows

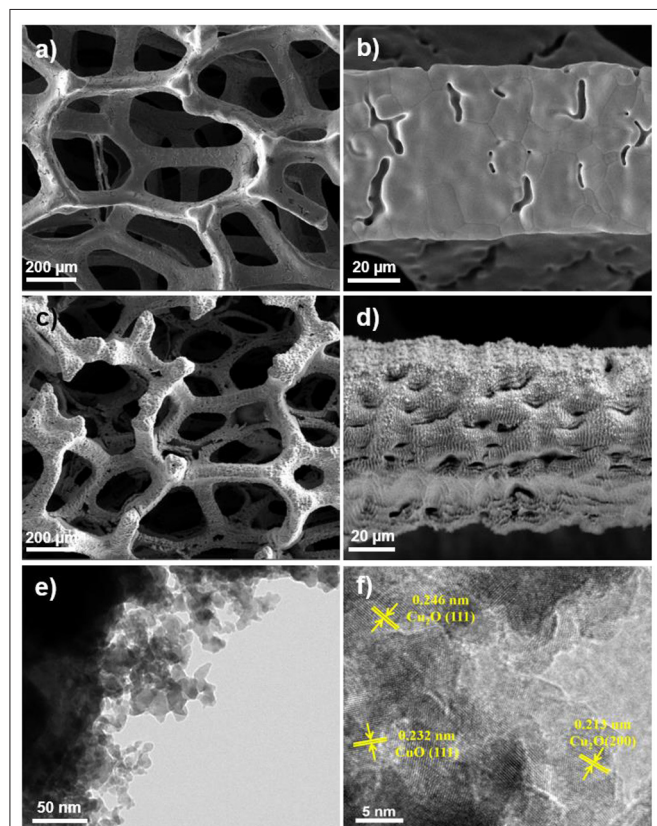


**FIGURE 1** | (a,b) SEM images of pristine Cu foam. (c,d) SEM images of the laser fabricated Cu foam. (e,f) TEM and HRTEM images of the laser fabricated Cu foam.

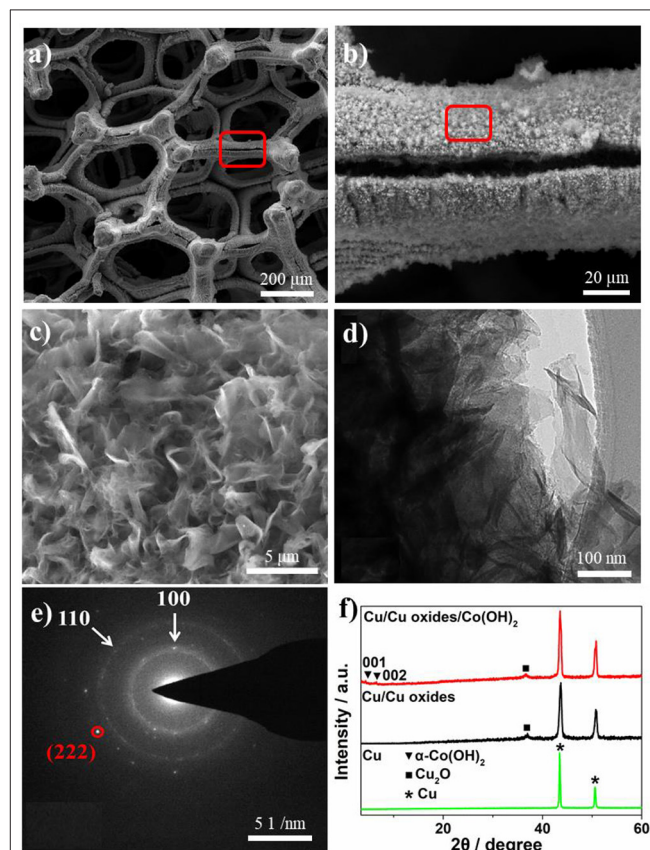


**FIGURE 2** | (a–c) SEM images of Cu/Cu oxides/Co(OH)<sub>2</sub>-8 h sample with different magnifications. (d) TEM and (e) SAED pattern images of Cu/Cu oxides/Co(OH)<sub>2</sub>-8 h. (f) XRD of the pristine Cu foam, laser fabricated Cu foam, and Cu/Cu oxides/Co(OH)<sub>2</sub>-8 h.

that the BET specific surface area of pristine Cu foam is  $0.22 \text{ m}^2/\text{g}$ , while that of laser ablated Cu foam increases to  $0.98 \text{ m}^2/\text{g}$ , indicating the formation of micro/nano-structures. **Figure S1** presents the water wettability of the pristine and the laser ablated Cu foam, which confirms the superhydrophilicity of the laser ablated Cu foam.

After the growth of  $\text{Co}(\text{OH})_2$ , clear layered  $\text{Co}(\text{OH})_2$  nanosheets were found on the laser fabricated Cu surface with a lateral dimension of a few hundreds of nanometers to a few micrometers (**Figures 2a–d**). The two ordered diffraction rings of the selected area electron diffraction (SAED) pattern can be assigned to (100) and (110) of  $\text{Co}(\text{OH})_2$  (**Figure 2e**; Liu et al., 2014), where one can also see diffraction patterns of  $\text{Cu}_2\text{O}$ , i.e., (222). **Figure 2f** shows the X-ray diffraction pattern of different samples. The pristine Cu foam only contains the characteristic peaks of bare Cu, while the laser ablation induced the formation of Cu oxides, corresponding to the (111) of  $\text{Cu}_2\text{O}$  (JCPDS 78-2076). No clear CuO peak can be found in the XRD pattern, probably due to the low content in the samples. After the precipitation conversion, two small peaks appear around  $4.5^\circ$  and  $6.5^\circ$ , which can be assigned to the (001) and (002) planes of  $\alpha\text{-Co}(\text{OH})_2$ , respectively (Liu et al., 2014). The existence of Cu, Co, and O elements is further confirmed by the energy dispersive X-ray (EDX) elemental mapping images (**Figure S2**).

XPS measurements were performed to identify the chemical valence states of the different elements in the samples. The

pristine Cu foam shows slight surface oxidation, while the laser ablation not only creates rich micro/nano-structures but also accelerates the oxidation with a sharp increase of the  $\text{Cu}^{1+}$  peak (**Figure 3a**) and a broadened O 1s peak (**Figure 3b**). After the precipitation conversion, the abrupt increase of  $\text{Cu}^{2+}$  peak

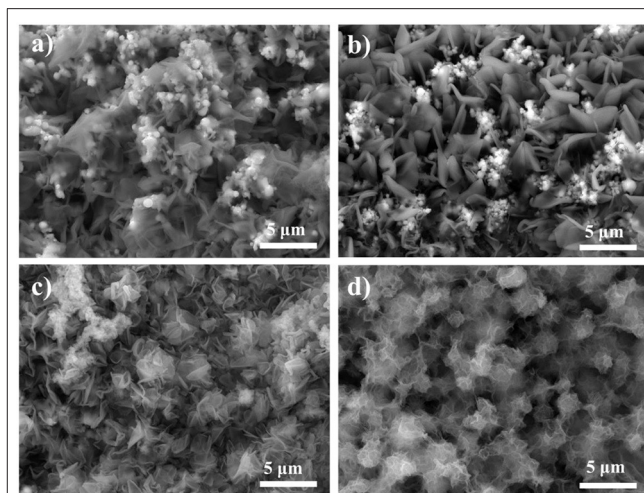


**FIGURE 4** | SEM images of the synthesized samples with different reaction time in the reactor **(a)** 2 h, **(b)** 4 h, **(c)** 6 h, and **(d)** 10 h.

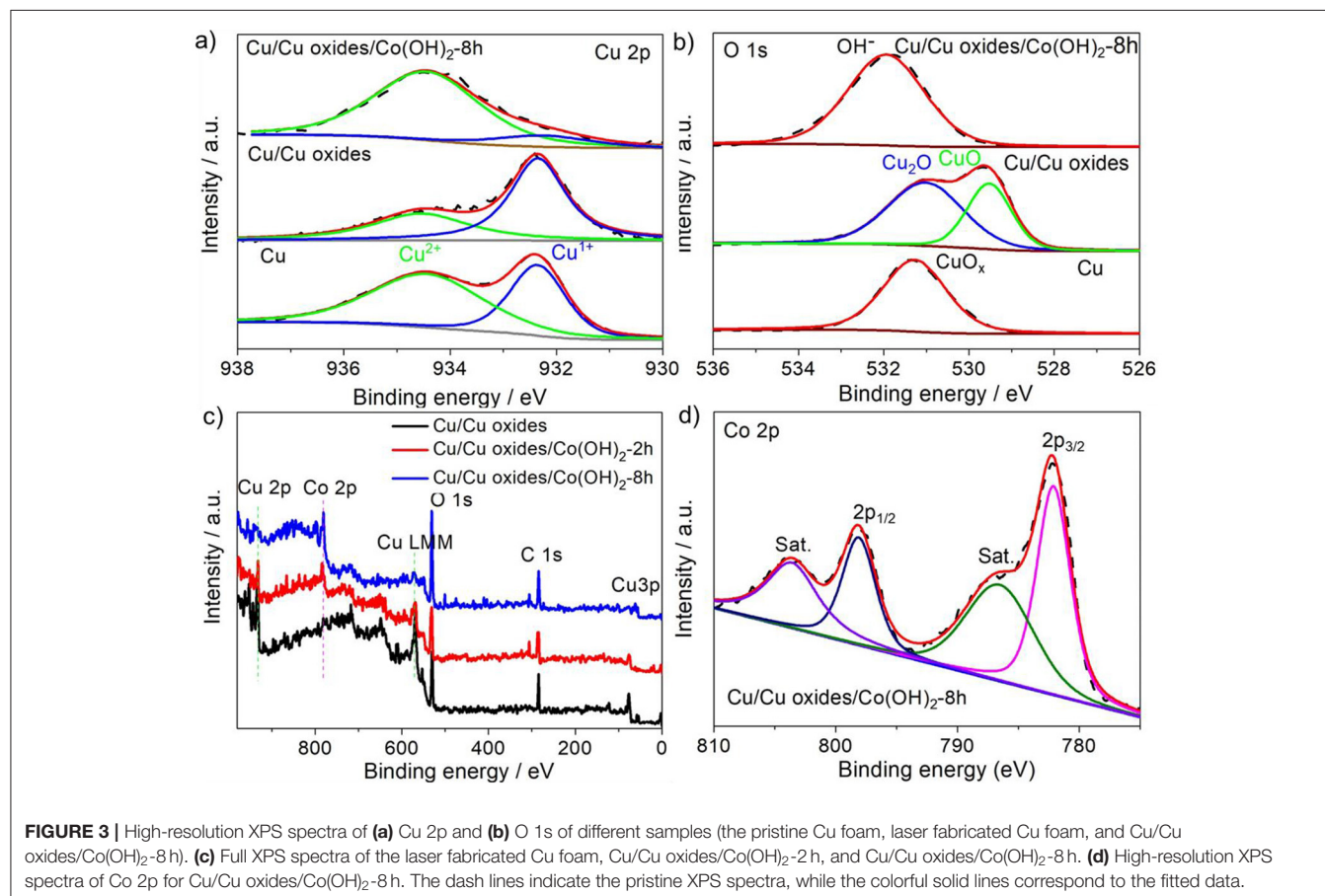
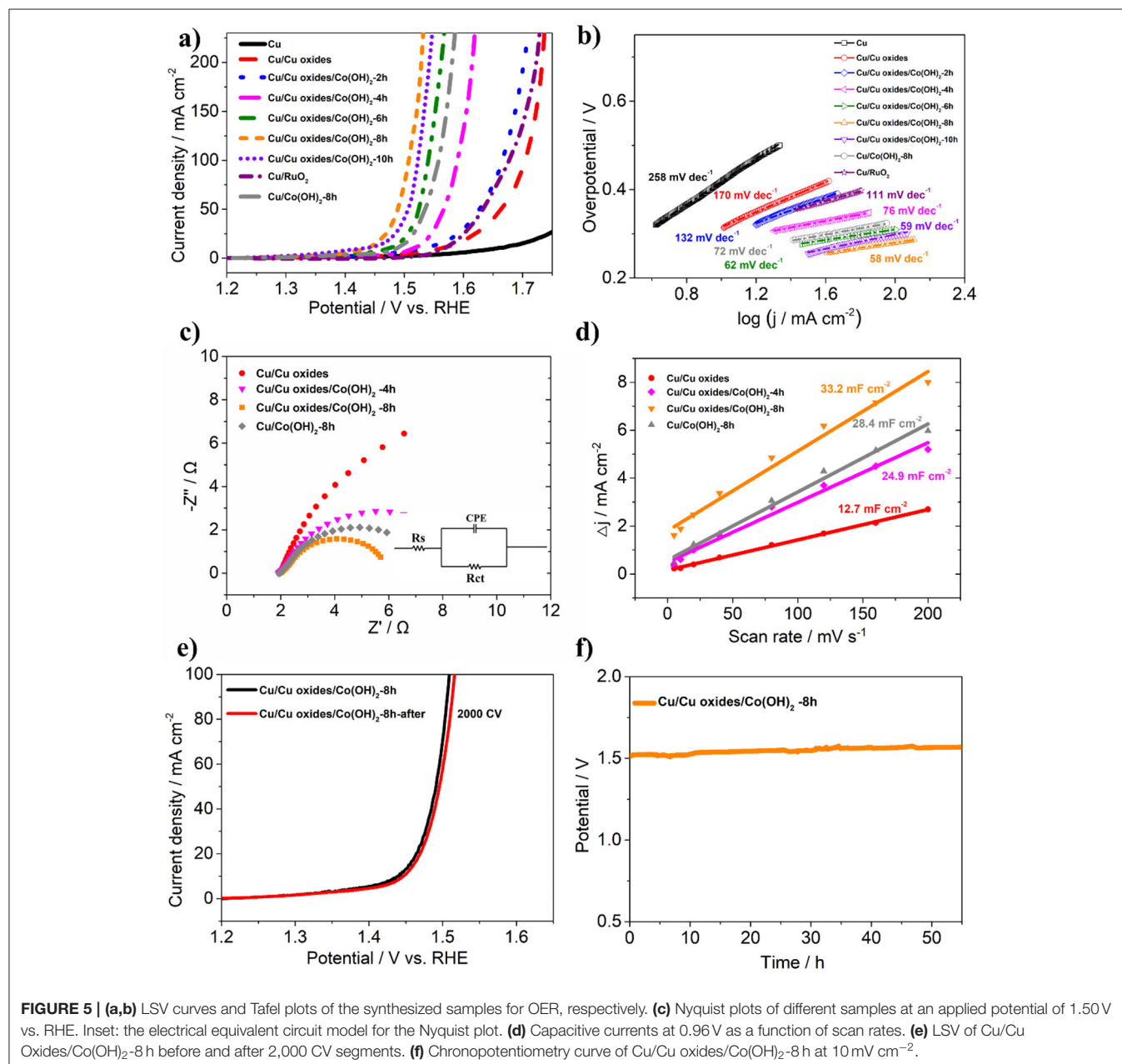


**FIGURE 3** | High-resolution XPS spectra of **(a)** Cu 2p and **(b)** O 1s of different samples (the pristine Cu foam, laser fabricated Cu foam, and Cu/Cu oxides/ $\text{Co}(\text{OH})_2$ -8 h). **(c)** Full XPS spectra of the laser fabricated Cu foam, Cu/Cu oxides/ $\text{Co}(\text{OH})_2$ -2 h, and Cu/Cu oxides/ $\text{Co}(\text{OH})_2$ -8 h. **(d)** High-resolution XPS spectra of Co 2p for Cu/Cu oxides/ $\text{Co}(\text{OH})_2$ -8 h. The dash lines indicate the pristine XPS spectra, while the colorful solid lines correspond to the fitted data.

indicates a further oxidation of surface  $\text{Cu}_2\text{O}$  to  $\text{CuO}$  during the process. The successful growth of  $\text{Co}(\text{OH})_2$  is verified by the appearance of  $\text{OH}^-$  in the O 1s spectra and Co 2p peak, and the gradual disappearance of the Cu peak (Figures 3b,c). The Co 2p peak splits into 2p 1/2 and 2p 3/2 located at 798.0 and 782.1 eV (Figure 3d), with a spin orbital splitting energy of about 16 eV, in agreement with the binding energies for the  $\text{Co}^{2+}$  oxidation state (Jiang et al., 2016). Moreover, the shake-up peak of Co 2p<sub>3/2</sub> further confirms the existence of  $\text{Co}^{2+}$ .

Since the catalytic activity of the electrocatalysts depends on the morphology, the laser fabricated Cu foams were placed in the reactor with different reaction time (2, 4, 6, 8, and 10 h) under the same condition, in order to explore the reaction time

dependent morphology evolution, which is characterized by SEM (Figure 4). In general, the amount of  $\text{Co}(\text{OH})_2$  increases with the increasing of reaction time (See more SEM images with different magnifications in Figures S3–S6). For Cu/Cu oxides/ $\text{Co}(\text{OH})_2$ -2 h, the laser fabricated Cu foam was partially coated with  $\text{Co}(\text{OH})_2$  nanosheets, where one can still see Cu oxide microstructures. Increasing the reaction time up to 8 h (Figure 2c), the sample is completely covered by  $\text{Co}(\text{OH})_2$  nanosheets from the SEM images. Further increasing the reaction time only results in the overgrowth of  $\text{Co}(\text{OH})_2$  on the surface with clear agglomeration. This is consistent with the XPS results. As shown in Figure 3c, with the increasing of preparation time, the Co 2p peak increases, while the Cu 2p and Cu LMM peaks decrease, indicating the gradual growth of  $\text{Co}(\text{OH})_2$  on the foams.



To further evaluate the OER performance, the prepared samples were tested in 1 M KOH using a standard three-electrode setup. From the LSV polarization curves (Figure 5a), it is shown that the laser ablated Cu foams possess certain OER activity due to the fabricated rich micro/nano-structures, compared to the pristine Cu foams. After the growth of  $\text{Co}(\text{OH})_2$ , the synthesized samples show clearly enhanced OER activity. In consistent with the morphology evolution as demonstrated in Figure 4, the OER activity of the samples rises with the increasing of the reaction time, while the overgrowth of  $\text{Co}(\text{OH})_2$  only results in a declined activity due to the decreased active sites as well as an increased resistance (Jiang et al., 2016). Among them, Cu/Cu oxides/ $\text{Co}(\text{OH})_2$ -8 h exhibits the best OER activity, with an overpotential of only 259 mV at  $50 \text{ mA cm}^{-2}$  and a Tafel slope of  $58 \text{ mV dec}^{-1}$  (Figures 5a,b), much smaller than those of the other samples. This activity is comparable or superior to the similar OER electrocatalysts reported in literature (Table S1; Jiang et al., 2016; Liu et al., 2016; Han et al., 2017; Huan et al., 2017; Zhang et al., 2017; Czioska et al., 2018; Li et al., 2018). For comparison,  $\text{Co}(\text{OH})_2$  nanosheets are also grown on pristine Cu foam ( $\text{Cu}/\text{Co}(\text{OH})_2$ -8 h) with an overpotential of 305 mV at  $50 \text{ mA cm}^{-2}$  and Tafel slope of  $72 \text{ mV dec}^{-1}$ , much larger than these of Cu/Cu oxides/ $\text{Co}(\text{OH})_2$ -8 h. Moreover, the effect of laser speed on the OER performance of the samples (Figure S7) is also investigated, where it is obvious that the 3 m/s sample shows better catalytic performance. It can be due to the more micro/nano-structures induced during the slow laser ablation process, which thus increases the growth sites for  $\text{Co}(\text{OH})_2$  as well as the active sites for the reactivity. However, one should also note that the Cu foams can be damaged if the scanning speed is too slow. To compare with, commercial  $\text{RuO}_2$  shows an overpotential of 400 mV at  $50 \text{ mA cm}^{-2}$  and Tafel slope of  $111 \text{ mV dec}^{-1}$ , also much larger than these of Cu/Cu oxides/ $\text{Co}(\text{OH})_2$ -8 h. According to the reaction pathway proposed by Krasil'shchikov (Doyle and Lyons, 2016), the Cu/Cu oxides/ $\text{Co}(\text{OH})_2$ -8 h have a Tafel slope of  $58 \text{ mV dec}^{-1}$ , indicating that the second electron transfer process, i.e.,  $\text{MO}^- \rightarrow \text{MO} + e^-$ , maybe the rate-determining step (RDS) of OER generation. To further understand the catalytic performance, electrochemical impedance spectroscopy was carried out (Figure 5c) and the fitted results of Nyquist plot are shown in Table S2, where Cu/Cu oxides/ $\text{Co}(\text{OH})_2$ -8 h has the smallest semicircle radius, indicating faster catalytic kinetics. Figure 5d depict the capacitance (normalized by the area) estimated by cyclic voltammetry (CV) curves measured at different scan rates for different samples (Figure S8). It is clearly shown that the capacitance of Cu/Cu oxides/ $\text{Co}(\text{OH})_2$ -8 h ( $33.2 \text{ mF cm}^{-2}$ ) is larger than that of Cu/Cu oxides ( $12.7 \text{ mF cm}^{-2}$ ), Cu/Cu oxides/ $\text{Co}(\text{OH})_2$ -4 h ( $24.9 \text{ mF cm}^{-2}$ ), and Cu/ $\text{Co}(\text{OH})_2$ -8 h ( $28.4 \text{ mF cm}^{-2}$ ) due to the growth of  $\text{Co}(\text{OH})_2$  and the increased active sites from laser ablation.

To evaluate the mild-term durability of the prepared electrocatalysts, the LSV after 2,000 CV of Cu/Cu oxides/ $\text{Co}(\text{OH})_2$ -8 h was tested. As shown in Figure 5e, the overpotential only shows an increase of 5 mV at  $50 \text{ mA cm}^{-2}$  after the test. Chronopotentiometry test was carried out to further confirm the good long-term stability (Figure 5f), where

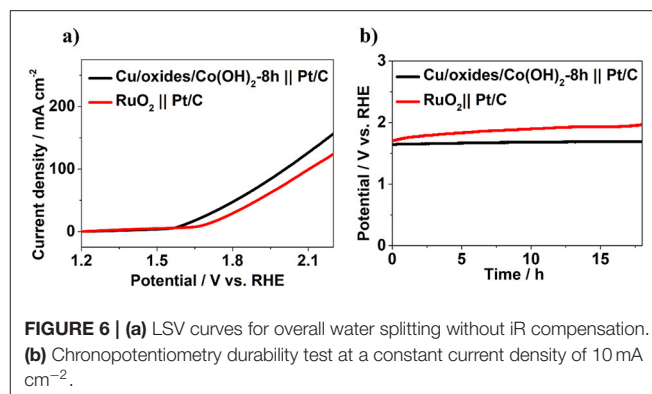


**FIGURE 6 |** (a) LSV curves for overall water splitting without iR compensation. (b) Chronopotentiometry durability test at a constant current density of  $10 \text{ mA cm}^{-2}$ .

the potential of Cu/Cu oxides/ $\text{Co}(\text{OH})_2$ -8 h does not show obvious increase after about 55 h at  $10 \text{ mA cm}^{-2}$ . In addition, both TEM and SEM images demonstrate that the morphology of the samples retains without significant changes after reaction (Figures S9, S10), confirming its excellent mild-term stability. The Faradaic efficiency (FE) of Cu/Cu Oxides/ $\text{Co}(\text{OH})_2$ -8 h was carried out together with the gas chromatography experiment (see details in Figure S11). We conduct the experiment with two voltages (1.51 and 1.55 V vs. RHE), where the corresponding FE are estimated to be 96.5 and 98.4%.

To further evaluate the possibility of Cu/Cu oxides/ $\text{Co}(\text{OH})_2$  for practical utilization, a water splitting system was built with Cu/Cu oxides/ $\text{Co}(\text{OH})_2$ -8 h and commercial Pt/C as anode and cathode, respectively. In comparison with the commercial  $\text{RuO}_2$  || Pt/C (Figure 6), the Cu/Cu oxides/ $\text{Co}(\text{OH})_2$ -8 h || Pt/C system displays a lower overpotential to reach  $10 \text{ mA cm}^{-2}$  (371 mV compared to 451 mV). For chronopotentiometry durability test, the  $\text{RuO}_2$  || Pt/C system shows a clear increase of potential with time, while that of the Cu/Cu oxides/ $\text{Co}(\text{OH})_2$ -8 h || Pt/C system stays up to 18 h, indicating better mild-term durability. In general, the enhanced OER activity of the laser fabricated samples can be attributed to the following reasons: (1) The produced Cu oxides have certain OER activity, compared to bare Cu foam. (2) The laser fabricated Cu surfaces with rich micro/nano-structures and large surface area are helpful for the growth of  $\text{Co}(\text{OH})_2$  nanosheets, thus with more active sites. (3) The fabricated micro/nano-structures possess certain porosity and are superhydrophilic, which can be conducive to the diffusion of water molecules and to the release of gas molecules thus fast OER kinetics for the prepared catalysts.

## CONCLUSIONS

In summary, a highly active OER electrocatalyst, i.e., Cu/Cu oxides/ $\text{Co}(\text{OH})_2$ , has been successfully synthesized through a combination of laser fabrication and precipitation conversion method. It only requires a low overpotential of 259 mV to reach a current density of  $50 \text{ mA cm}^{-2}$  in 1 M KOH, associated with superior durability of more than 55 h and a small Tafel slope of  $58 \text{ mV dec}^{-1}$ , due to significantly improved active sites and the superhydrophilicity from the laser fabrication. Our study

provides a new strategy to the design and construction of high efficient non-noble metal based OER catalysts.

## DATA AVAILABILITY STATEMENT

All datasets generated for this study are included in the article/**Supplementary Material**.

## AUTHOR CONTRIBUTIONS

XZ carried out the experiments and data analysis, as well as wrote the manuscript. KY modified the substrates with laser ablation. WQ and YL co-designed the experiments. WQ, NZ, SG, ZL, and YL discussed the experimental data and revised the manuscript together.

## FUNDING

This work was supported by National Natural Science Foundation of China (Grant No. 11904411), the Fundamental

Research Funds for the Central Universities (Grant No.31020195C001), Natural Science Basic Research Program of Shanxi Province (Grant No. 2019JM-192), Natural Science Foundation of Hunan Province (Grant No. 2018JJ3626), and the Open Sharing Fund for the Large-scale Instruments and Equipment of Central South University.

## SUPPLEMENTARY MATERIAL

The Supplementary Material for this article can be found online at: <https://www.frontiersin.org/articles/10.3389/fchem.2019.00900/full#supplementary-material>

The supporting information includes: EDS mapping images of the synthesized Cu/Cu oxides/Co(OH)<sub>2</sub> electrocatalysts, SEM images and CVs of the synthesized catalysts, TEM and SEM images of the Cu/Cu Oxides/Co(OH)<sub>2</sub>-8 h after reaction, detailed information of gas chromatography experiment, the fitted results of the Nyquist plot, comparison of OER performances with literature results.

## REFERENCES

- Ai, L., Tian, T., and Jiang, J. (2017). Ultrathin graphene layers encapsulating nickel nanoparticles derived metal-organic frameworks for highly efficient electrocatalytic hydrogen and oxygen evolution reactions. *ACS Sustain. Chem. Eng.* 5, 4771–4777. doi: 10.1021/acsschemeng.7b00153
- Czioska, S., Wang, J., Zuo, S., Teng, X., and Chen, Z. (2018). Hierarchically structured NiFeOx/CuO nanosheets/nanowires as an efficient electrocatalyst for the oxygen evolution reaction. *ChemCatChem* 10, 1005–1011. doi: 10.1002/cctc.201701441
- Doyle, R. L., and Lyons, M. E. G. (2016). “The oxygen evolution reaction: mechanistic concepts and catalyst design,” in *Photoelectrochemical SolarFuel Production*, Vol. 2, eds S. Gimenez and J. Bisquert (Berlin: Springer), 41–104. doi: 10.1007/978-3-319-29641-8\_2
- Duan, J. A., Dong, X., Yin, K., Yang, S., and Chu, D. (2018). A hierarchical superaerophilic cone: robust spontaneous and directional transport of gas bubbles. *Appl. Phys. Lett.* 113:203704. doi: 10.1063/1.5054623
- Gong, M., Li, Y., Wang, H., Liang, Y., Wu, J. Z., Zhou, J., et al. (2013). An advanced Ni-Fe layered double hydroxide electrocatalyst for water oxidation. *J. Am. Chem. Soc.* 135, 8452–8455. doi: 10.1021/ja4027715
- Han, A., Zhang, H., Yuan, R., Ji, H., and Du, P. (2017). Crystalline copper phosphide nanosheets as an efficient janus catalyst for overall water splitting. *ACS Appl. Mater. Interfaces* 9, 2240–2248. doi: 10.1021/acsami.6b10983
- Huan, T. N., Rouse, G., Zanna, S., Lucas, I. T., Xu, X., Menguy, N., et al. (2017). A dendritic nanostructured copper oxide electrocatalyst for the oxygen evolution reaction. *Angew. Chem. Int. Ed.* 56, 4792–4796. doi: 10.1002/anie.201700388
- Jiang, Y., Li, X., Wang, T., and Wang, C. (2016). Enhanced electrocatalytic oxygen evolution of  $\alpha$ -Co(OH)<sub>2</sub> nanosheets on carbon nanotube/polyimide films. *Nanoscale* 8, 9667–9675. doi: 10.1039/C6NR00614K
- Jin, H., Mao, S., Zhan, G., Xu, F., Bao, X., and Wang, Y. (2017). Fe incorporated  $\alpha$ -Co(OH)<sub>2</sub> nanosheets with remarkably improved activity towards the oxygen evolution reaction. *J. Mater. Chem. A* 5, 1078–1084. doi: 10.1039/C6TA09959A
- Jin, J., Ouyang, J., and Yang, H. (2017). Pd nanoparticles and MOFs synergistically hybridized halloysite nanotubes for hydrogen storage. *Nanoscale Res. Lett.* 12:240. doi: 10.1186/s11671-017-2000-5
- Lee, Y., Suntivich, J., May, K. J., Perry, E. E., and Shao-Horn, Y. (2012). Synthesis and activities of rutile IrO<sub>2</sub> and RuO<sub>2</sub> nanoparticles for oxygen evolution in acid and alkaline solutions. *J. Phys. Chem. Lett.* 3, 399–404. doi: 10.1021/jz2016507
- Li, A., Wang, C., Zhang, H., Zhao, Z., Wang, J., Cheng, M., et al. (2018). Cobalt oxide (Co<sub>3</sub>O<sub>4</sub>) for oxygen evolution reaction. *Electrochim. Acta* 276, 153–161. doi: 10.1016/j.electacta.2018.04.177
- Li, X., Hao, X., and Guan, G. (2016). Nanostructured catalysts for electrochemical water splitting: current state and prospects. *J. Mater. Chem. A* 4, 11973–12000. doi: 10.1039/C6TA02334G
- Li, Y., Pei, W., He, J., Liu, K., Qi, W., Gao, X., et al. (2019a). Hybrids of PtRu nanoclusters and black phosphorus nanosheets for highly efficient alkaline hydrogen evolution reaction. *ACS Catal.* 9, 10870–10875. doi: 10.1021/acscatal.9b03506
- Li, Y., Zhou, X., Qi, W., Xie, H., Yin, K., Tong, Y., et al. (2019b). Ultrafast fabrication of Cu oxide micro/nano-structures via laser ablation to promote oxygen evolution reaction. *Chem. Eng. J.* doi: 10.1016/j.cej.2019.123086. [Epub ahead of print].
- Liu, P., Liu, X., Lyu, L., Xie, H., Zhang, H., Niu, D., et al. (2015). Interfacial electronic structure at the CH<sub>3</sub>NH<sub>3</sub>PbI<sub>3</sub>/MoO<sub>x</sub> interface. *Appl. Phys. Lett.* 106:193903. doi: 10.1063/1.4921339
- Liu, P. F., Yang, S., Zheng, L. R., Zhang, B., and Yang, H. G. (2016). Electrochemical etching of  $\alpha$ -cobalt hydroxide for improvement of oxygen evolution reaction. *J. Mater. Chem. A* 4, 9578–9584. doi: 10.1039/C6TA04078K
- Liu, X., Ma, R., Bando, Y., and Sasaki, T. (2014). High-yield preparation, versatile structural modification, and properties of layered cobalt hydroxide nanocones. *Adv. Funct. Mater.* 24, 4292–4302. doi: 10.1002/adfm.201400193
- Liu, Y., Zai, H., Xie, H., Liu, B., Wang, S., Zhao, Y., et al. (2019). Effects of CsPbBr<sub>3</sub> nanocrystals concentration on electronic structure and surface composition of perovskite films. *Org. Electron.* 73, 327–331. doi: 10.1016/j.orgel.2019.06.040
- Lu, X. F., Liao, P. Q., Wang, J. W., Wu, J. X., Chen, X. W., He, C. T., et al. (2016). An alkaline-stable, metal hydroxide mimicking metal-organic framework for efficient electrocatalytic oxygen evolution. *J. Am. Chem. Soc.* 138, 8336–8339. doi: 10.1021/jacs.6b03125
- Lv, L., Yang, Z., Chen, K., Wang, C., and Xiong, Y. (2019). 2D layered double hydroxides for oxygen evolution reaction: from fundamental design to application. *Adv. Energy Mater.* 9:1803358. doi: 10.1002/aenm.201803358
- Ma, W., Ma, R., Wu, J., Sun, P., Liu, X., Zhou, K., et al. (2016). Development of efficient electrocatalysts: via molecular hybridization of NiMn layered double hydroxide nanosheets and graphene. *Nanoscale* 8, 10425–10432. doi: 10.1039/C6NR00988C
- Meng, C., Wang, B., Gao, Z., Liu, Z., Zhang, Q., and Zhai, J. (2017). Insight into the role of surface wettability in electrocatalytic hydrogen evolution reactions using light-sensitive nanotubular TiO<sub>2</sub> supported Pt electrodes. *Sci. Rep.* 7, 1–8. doi: 10.1038/srep41825

- Shi, Y., and Zhang, B. (2016). Recent advances in transition metal phosphide nanomaterials: synthesis and applications in hydrogen evolution reaction. *Chem. Soc. Rev.* 45, 1529–1541. doi: 10.1039/C5CS00434A
- Sivanantham, A., Ganesan, P., and Shanmugam, S. (2016). Hierarchical NiCo<sub>2</sub>S<sub>4</sub> nanowire arrays supported on Ni Foam: an efficient and durable bifunctional electrocatalyst for oxygen and hydrogen evolution reactions. *Adv. Funct. Mater.* 26, 4661–4672. doi: 10.1002/adfm.201600566
- Wu, H., Yin, K., Qi, W., Zhou, X., He, J., Li, J., et al. (2019). Rapid fabrication of Ni/NiO@CoFe layered double hydroxide hierarchical nanostructures by femtosecond laser ablation and electrodeposition for efficient overall water splitting. *ChemSusChem* 12, 2773–2779. doi: 10.1002/cssc.201900479
- Wu, N., Lei, Y., Wang, Q., Wang, B., Han, C., and Wang, Y. (2017). Facile synthesis of FeCo@NC core-shell nanospheres supported on graphene as an efficient bifunctional oxygen electrocatalyst. *Nano Res.* 10, 2332–2343. doi: 10.1007/s12274-017-1428-3
- Xia, B. Y., Yan, Y., Li, N., Wu, H., Bin, Lou, X. W. D., and Wang, X. (2016). A metal-organic framework-derived bifunctional oxygen electrocatalyst. *Nat. Energy* 1:15006. doi: 10.1007/978-981-10-0218-2
- Xie, H., Niu, D., Lyu, L., Zhang, H., Zhang, Y., Liu, P., et al. (2016). Evolution of the electronic structure of C<sub>60</sub>/La<sub>0.67</sub>Sr<sub>0.33</sub>MnO<sub>3</sub> interface. *Appl. Phys. Lett.* 108:011603. doi: 10.1063/1.4939457
- Xie, L., Tang, C., Wang, K., Du, G., Asiri, A. M., and Sun, X. (2017). Cu(OH)<sub>2</sub>@CoCO<sub>3</sub>(OH)<sub>2</sub>·nH<sub>2</sub>O core-shell heterostructure nanowire array: an efficient 3D anodic catalyst for oxygen evolution and methanol electrooxidation. *Small* 13:1602755. doi: 10.1002/smll.201602755
- Xiong, X., You, C., Liu, Z., Asiri, A. M., and Sun, X. (2018). Co-doped CuO nanoarray: an efficient oxygen evolution reaction electrocatalyst with enhanced activity. *ACS Sustain. Chem. Eng.* 6, 2883–2887. doi: 10.1021/acssuschemeng.7b03752
- Yang, S., Yin, K., Chu, D., He, J., and Duan, J. A. (2018). Femtosecond laser structuring of Janus foam: water spontaneous antigravity unidirectional penetration and pumping. *Appl. Phys. Lett.* 113:203701. doi: 10.1063/1.5061723
- Yin, K., Chu, D., Dong, X., Wang, C., Duan, J. A., and He, J. (2017a). Femtosecond laser induced robust periodic nanoripple structured mesh for highly efficient oil-water separation. *Nanoscale* 9, 14229–14235. doi: 10.1039/C7NR04582D
- Yin, K., Du, H., Dong, X., Wang, C., Duan, J. A., and He, J. (2017b). A simple way to achieve bioinspired hybrid wettability surface with micro/nanopatterns for efficient fog collection. *Nanoscale* 9, 14620–14626. doi: 10.1039/C7NR05683D
- Zhang, L., Zhang, R., Ge, R., Ren, X., Hao, S., Xie, F., et al. (2017). Facilitating active species generation by amorphous NiFe-BiLayer formation on NiFe-LDH nanoarray for efficient electrocatalytic oxygen evolution at alkaline pH. *Chem. A Eur. J.* 23, 11499–11503. doi: 10.1002/chem.201702745

**Conflict of Interest:** The authors declare that the research was conducted in the absence of any commercial or financial relationships that could be construed as a potential conflict of interest.

Copyright © 2020 Zhou, Qi, Yin, Zhang, Gong, Li and Li. This is an open-access article distributed under the terms of the Creative Commons Attribution License (CC BY). The use, distribution or reproduction in other forums is permitted, provided the original author(s) and the copyright owner(s) are credited and that the original publication in this journal is cited, in accordance with accepted academic practice. No use, distribution or reproduction is permitted which does not comply with these terms.